Small-Molecule Stabilization Mechanisms of Metal Oxide Nanoparticles

S. Zellmer, C. Grote, T.A. Cheema and G. Garnweitner

Abstract The stabilization of nanoparticles to prevent agglomeration is of great importance for their application. To achieve long-term stable particle dispersions that can be stored and processed, and to clarify stabilization mechanisms in detail, the stabilization of metal oxide nanoparticles with small molecules was investigated. Particularly, the adsorption of the stabilizer and thereby the dynamic and kinetic processes on the surface of the metal oxide nanoparticles are essential for the stabilization process. Within this project, particle-stabilizer-solvent-interactions for different particle systems, ITO and ZrO_2, were described and influences of the chain length, the stabilizer concentration as well as the binding strength between stabilizer and surface were investigated and modeled. The developed model enables a prediction of the efficiency of the systems and about optimized combinations of stabilizer-particle-solvent systems.

Keywords Metal oxide nanoparticles · Colloidal stability · Stabilization mechanisms · Steric stabilization · Non-aqueous sol-gel synthesis

1 Introduction

Based on their unique properties, metal oxide nanoparticles are used in a variety of applications. ITO nanoparticles, for example, belong to the class of transparent conducting oxides (TCO) and show promise in the field of printable electronics for cheap and reliable polymer-based flexible touch-panels as well as displays [1–3]. As another example, ZrO_2 nanoparticles are highly attractive for ceramics,

S. Zellmer (✉) · C. Grote · T.A. Cheema · G. Garnweitner
TU Braunschweig, Institut für Partikeltechnik, Volkmaroder Str. 5,
38104 Braunschweig, Germany
e-mail: s.zellmer@tu-bs.de

G. Garnweitner
e-mail: g.garnweitner@tu-bs.de

M. Kind et al. (eds.), *Colloid Process Engineering*,
DOI 10.1007/978-3-319-15129-8_4

coatings, electronic devices, thin film capacitors and composites because of their enhanced mechanical and dielectric properties [4–13].

To process and utilize these materials in different fields, the nanoparticles must be stabilized to prevent agglomeration. The combination of attractive interactions, such as van der Waals forces, and repulsive interactions determines whether the particles will agglomerate. These repulsive interactions can be achieved by steric repulsion via the adsorption of organic molecules on the particle surface or electrostatic repulsions caused by surface charges. To describe these stabilization mechanisms in detail, interactions between the particles, the particle and the stabilizer as well as the interactions between the stabilizer and the solvent must be considered [22–25].

In the last years, nanoparticles with superior properties were obtained from the syntheses in hot organic media. Whilst, in many cases, surfactants are present and result in instant stabilization, their selection is arbitrary and empirical, and often large excess of organics is present in the final product. In other cases, only inert solvents are used and the particles consequently tend to agglomerate during the synthesis; however, they can be stabilized by the addition of surfactants. Generally, organic moieties from the synthesis are often present at the particle surface and it remains unclear whether these facilitate or hinder the stabilization as well as whether the stabilizer replaces these groups or adsorbs via additional binding sites at the particle surface. Additionally, in the case of nanoparticles less than 20 nm in size, stabilization can be achieved by the use of small molecules rather than polymer chains. Thereby, a decrease in the particle size leads to a smaller contribution of attractive particle interactions at a given distance, so that small molecules, such as surfactants, can prevent agglomeration [26–28, 33].

The influence of the organic layer thickness is often investigated by varying chain length of the stabilizer. For example, Bergström et al. [27] published the stabilization of Al_2O_3 particles with fatty acids of different chain lengths. Siffert et al. [29] stabilized TiO_2 nanoparticles with various n-alkylamines in nonpolar solvents. The results of these studies as well as the experiments from Sun et al. [30] and Marczak et al. [31] have shown that stabilization principally depends on the electrostatic and steric effects.

Furthermore, different models which describe the stabilization of nanoparticles in polar and nonpolar solvents were proposed in the literature. Segets et al. [32] modeled the colloidal stabilization of ZnO particles using dimensionless numbers as a function of the geometry as well as attractive and repulsive forces. In contrast to the DLVO theory, this allows for not only the calculation of energy barriers, but also the consideration of the whole stabilization process [32]. Still, the applicability of these models to nanoparticles prepared in hot organic media remains unclear.

Within this project, experimental results and theoretical models were combined to describe and predict the stabilization of metal oxide nanoparticles using small molecules. For the synthesis of well-defined highly crystalline metal oxide nanoparticles as model systems, the non-aqueous sol-gel synthesis was employed. This synthesis is an easily reproducible method that enables the control of the particle size as well as the morphology of the particles. To describe and model the stabilization with short molecules, such as amines or carboxylic acids, ITO and ZrO_2 nanoparticles were selected as model systems. To prevent influences of the in situ stabilization

on the particle formation and to obtain a more detailed understanding of the interrelation between the adsorption-desorption process on the particle surface and the deagglomeration of the nanoparticles, post-synthetic stabilization was selected.

The main focus of the project was the elucidation of particle-stabilizer-solvent interactions as a function of the binding strength, the chain length, the concentration of the stabilizers, the polarity of the solvents, and the surface configuration as well as the size and morphology of the metal oxide nanoparticles. Therefore, to characterize the stabilization kinetics, a number of analytical methods, such as thermogravimetric analysis, isothermal titration calorimetry, and spectroscopic methods, were combined.

To complement the experimental results, an empirical model was developed to predict particle-stabilizer-solvent interactions. The model allows for the consideration of different stabilizer properties, such as the chain length, the concentration and the binding strength of the stabilizer. Furthermore, the stabilization time and temperature as well as solvent and particle properties can be included in the model. Depending on these influences, the efficiency of the stabilization process for different particle system can be identified and used to optimize the combination of particle-stabilizer-solvent systems.

2 Experimental

ITO and ZrO_2 nanoparticles were synthesized via the non-aqueous sol-gel method using benzyl alcohol as the high boiling solvent [3, 14–16]. In accordance with Ba et al. [3], In(III) acetylacetonate (≥99.99 % trace metals basis, Aldrich) and Sn(IV) *tert*-butoxide (≥99.99 % trace metals basis, Aldrich) as molecular precursors were dissolved in the organic reaction medium to prepare highly crystalline ITO nanoparticles. In the case of ZrO_2, Zr(IV) *n*-propoxide in 1-propanol (70 wt%, Aldrich) was used as precursor [14–16]. The reaction solutions were transferred into Teflon-lined steel autoclaves (Parr Instr.) and heated to 200 °C for 24 h (ITO) and 220 °C for 96 h (ZrO_2).

To stabilize the nanoparticles after synthesis, the particles were separated from the reaction mixture by centrifugation and washed twice with chloroform (ITO) and ethanol (ZrO_2). For the post-synthetic stabilization, small organic molecules, such as n-alkylamines (ITO) and carboxylic acids (ZrO_2), with different chain lengths and in a variety of concentrations were added to the dispersed nanoparticles in chloroform. The reaction between the stabilizer and the particle surface is achieved through simple shaking for 24 h at room temperature. Typically, this results in instant disintegration of agglomerates. A fraction of the particles is stabilized at primary particle level (termed “stable particles”) whereas another fraction remains present as agglomerates in the µm range (termed “unstable particles”). To separate the stable and unstable particle fractions, the particle dispersion must be centrifuged at 8500 rpm for 15 min. After the separation of both fractions, the stable fraction was precipitated by adding an organic solvent. In the case of ITO nanoparticles, methanol (in a volume ratio of 1:1) and for ZrO_2, ethyl acetate

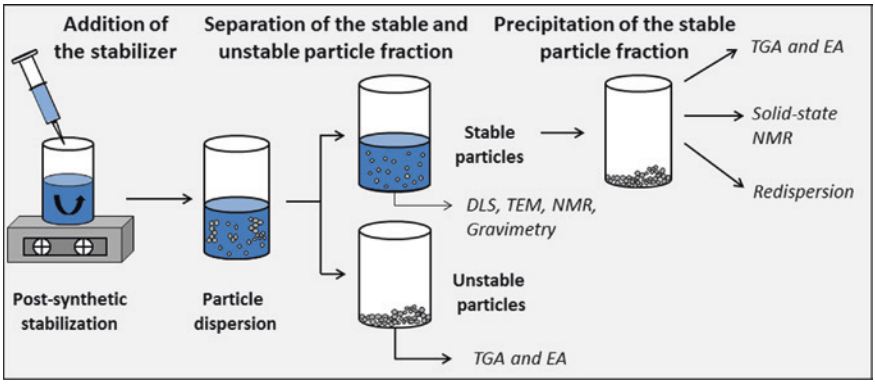

Fig. 1 Scheme of the stabilization process

(in a volume ratio of 5:1 ethyl acetate:dispersion) was used. The obtained precipitate was dried under vacuum at room temperature. The process scheme is plotted in Fig. 1.

To determine the particle size of the stable particle fraction of ITO and ZrO_2 nanoparticles, dynamic light scattering (Malvern Zetasizer Nano ZS) was used. The content of ITO and ZrO_2 nanoparticles in the dispersion was calculated using thermogravimetric analysis (TGA), which was performed on the dried powder samples and carried out on a Mettler Toledo TGA/SDTA 851 under oxygen flow in the range of 25–750 °C at 10 °C min^{-1}. To investigate the amount of the bound stabilizer in detail, elemental analysis (FlashEA 1112, ThermoQuest Italia S.p.A) was utilized. As spectroscopic methods, ^{13}C NMR spectroscopy (Bruker AV II-600) and solid-state-^{13}C-NMR (TU Paderborn, Tecmag, Apollo) were applied to verify the attachment of the stabilizer molecules. The quantification of the binding affinity was performed by isothermal reaction calorimetry (MPI Mainz, VP-ITC, Microcal. Inc., USA).

3 Results and Discussion

3.1 Particle Model Systems

ZrO_2 and ITO nanoparticles were prepared via the non-aqueous sol-gel synthesis. Thereby, highly crystalline and uniform nanoparticles were obtained; the synthesis is described in earlier works in detail [3, 14]. First, to show the differences between stable and unstable particle fractions, DLS measurements of the stable and unstable ITO particle fractions are exemplarily plotted in Fig. 2 left. After the particle synthesis, agglomerates with a particle size of approximately 1 µm for both particle systems were found; by using different stabilizers, particle sizes of approximately 10 nm for the ITO system (Fig. 2) and 5 nm for the ZrO_2 particle system (data not shown) were measured by DLS. This corresponds to the primary

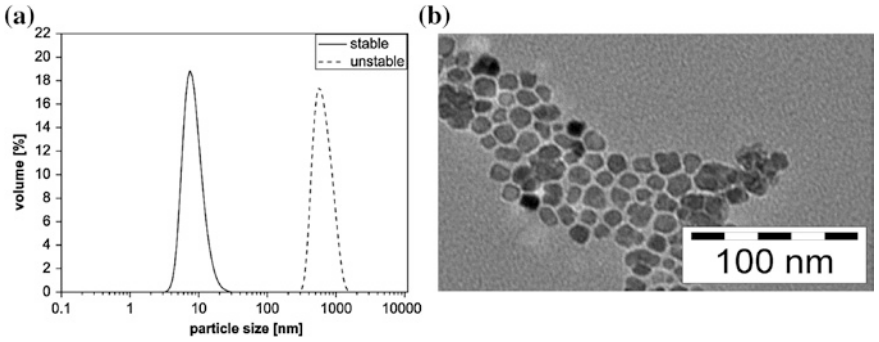

Fig. 2 DLS of a stable and unstable ITO nanoparticle fraction (*left*) and TEM image of ITO particles (*right*)

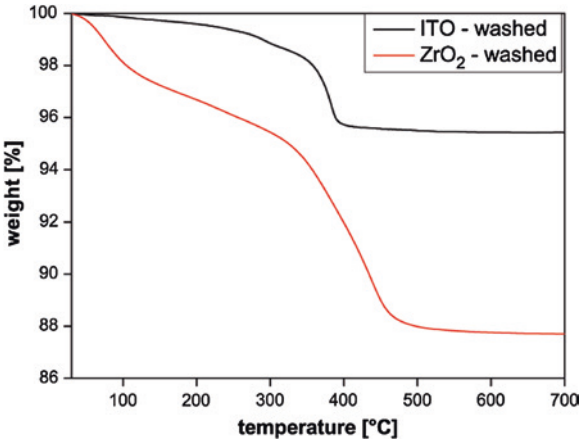

Fig. 3 TGA of ITO and ZrO_2 nanoparticles after washing

particle size of around 10 nm for ITO as shown by using TEM (Fig. 2, right) and 5 nm for ZrO_2 as presented in earlier works [17]. The TEM images also indicate similar particle morphologies, to be approximately spherical. For the further investigations, described in this work, DLS measurements were used to differentiate into stable and unstable particle fractions.

Gravimetric analyses of these synthesized ITO and ZrO_2 particles have shown that after a number of washing steps a constant amount of benzyl alcohol or alcohol derivatives are bound to the ITO and ZrO_2 particle surface. In the case of ITO around 5 wt% of benzyl alcohol is coupled to the particle surface; the TGA analysis of washed ZrO_2 nanoparticles shows an amount of around 10 wt% (Fig. 3). For both samples, washed ITO and ZrO_2 nanoparticles, the weight loss occurs in two steps. Thereby, the first step is attributed to weakly bound species such as volatile solvents; the second step at around 400 °C is assigned to chemisorbed benzyl alcohol and its side products. Based on the works of Zhou et al. [18] and Pinna et al. [19],

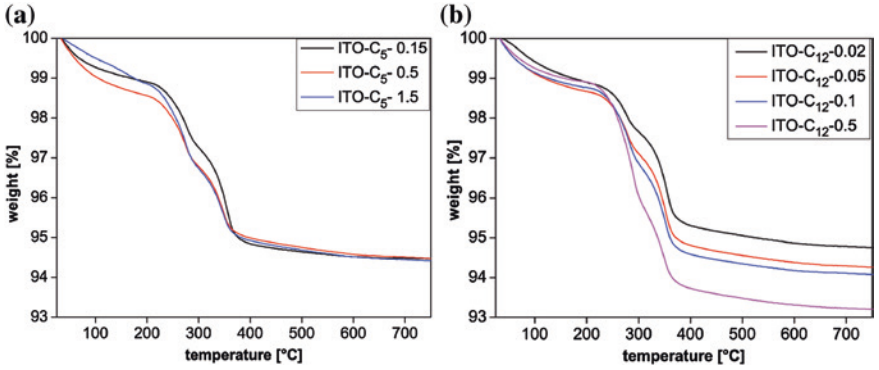

Fig. 4 TGA of ITO nanoparticles stabilized with the short-chain stabilizer amylamine (*left*) and the long-chain stabilizer dodecylamine (*right*)

we identified that in the case of ZrO_2 nanoparticles, benzoic acid was formed during the synthesis [16]. This change of the surface chemistry must be considered for further investigations and the elucidation of the stabilization of ZrO_2 particles.

3.2 Stabilization of Metal Oxide Nanoparticles

The absence of the stabilizer during the synthesis offers the possibility to investigate the dynamic and kinetic processes on the particle surface, both on a microscopic and macroscopic scale during the post-synthetic stabilization. The investigation of stabilization mechanisms furthermore involves the determination of particle, stabilizer and solvent influences.

First, to study the influence of stabilizer properties, such as the chain length, the amount of needed stabilizer and the binding strength, the other parameters, such as the temperature, the solvent as well as the stabilization time were kept constant. Therefore, depending on the affinity of the functional group of the stabilizer to the particle surface, ITO nanoparticles were stabilized with n-alkylamines of chain length between C_5 and C_{12} and the stabilization of ZrO_2 particles occurs upon the addition of carboxylic acids (C_6 to C_{12}).

3.3 Stabilization of ITO Nanoparticles with n-Alkylamines

For the stabilization of ITO nanoparticles, a variety of n-alkylamines with different chain length and added concentrations of the stabilizer in chloroform were applied. The TGA measurements plotted in Fig. 4 show strong differences between the short-chain stabilizer amylamine (left) and the long-chain stabilizer

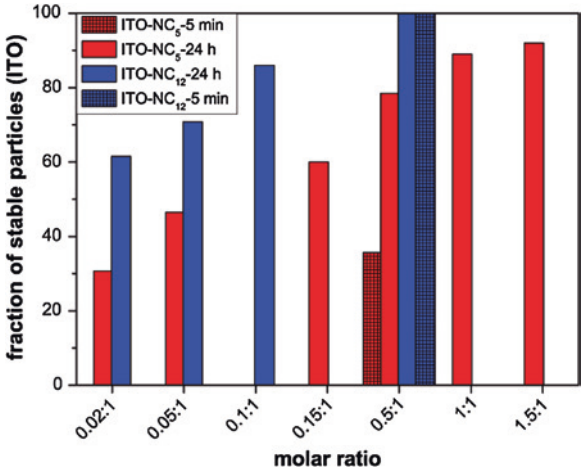

Fig. 5 Fraction of stabilized ITO nanoparticles as a function of different added stabilizer concentrations

dodecylamine (right). Thereby, the stable particle fractions were precipitated and dried prior to the measurements.

The addition of larger amounts of amylamine does not lead to an increase in the quantity of organics adsorbed to the particle surface. However, when higher amounts of dodecylamine were added to the dispersion, a continuous rise in the amount of bound stabilizer is observed. This points to a higher affinity of the long-chain stabilizer to the particle surface and results in different molar stabilizer-to-particle ratios required to stabilize 100 % of the particles in the system. In detail, the first weight-loss step is attributed to fragile bound volatile solvents; the second step is related to the bound stabilizer and the third step reflects the desorption of coupled benzyl alcohol from the particle surface [17].

To show the influence of the amount of added stabilizer on the stabilization, a range of concentrations were selected. In order to realize constant conditions, the amount of stable particles was measured after 24 h stirring in each experiment by separating the particle fractions. Figure 5 indicates the stable ITO content in % resulting from adding different molar ratios of the stabilizer.

As expected, an increase in the molar ratio leads to a higher amount of stable particles. In the case of dodecylamime, a value of 0.5:1 (stabilizer:ITO) is sufficient to stabilize 100 % of the particles in the experiment. Due to the strong influences of the chain length, higher amounts of amylamine are necessary for the stabilization. With the addition of 1.5:1 (stabilzer:ITO), around 90 % of the particles are stable [20].

Furthermore, to demonstrate the influence of the stabilization time, i.e. the period from the addition of the stabilizer until the investigation of the sample, the amount of stable particles after 5 min is additionally plotted for a molar ratio of 0.5:1 stabilizer to ITO nanoparticles. For the long chain stabilizer dodecylamine, 100 % of the particles were stabilized after 5 min stabilization time. In the case of the short chain stabilizer amylamine only 50 % of the particles, compared to the amount of stable particles after 24 h, could be stabilized [20].

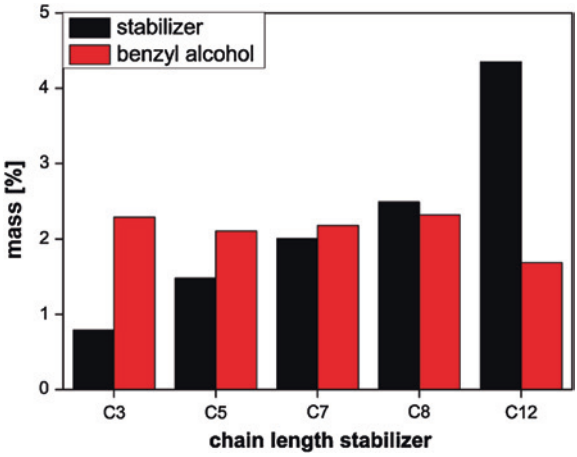

Fig. 6 Mass of the bound organics on the particle surface of stable ITO nanoparticles as determined by elemental analysis for stabilizers of different chain length

To show the stabilization mechanisms in detail, elemental analysis of the stable particle fractions was used to determine the amounts of benzyl alcohol and the stabilizer on the particle surface. Figure 6 indicates that, from the original 5 wt% benzyl alcohol adsorbed to the particle surface, about 2.5 wt% were desorbed with the adsorption of the stabilizer. Depending on the molecular weight of the stabilizer, the amount of bound stabilizer increases with the chain length; the amount of bound benzyl alcohol remains approximately constant.

To characterize the binding affinity of the n-alkylamines to the particle surface, isothermal titration calorimetry (MPI Mainz) combined with ^{13}C-NMR (TU Braunschweig) was applied. The attachment of the amines was analyzed with ^{13}C-NMR spectroscopy in order to show the selective interaction of the amine group with the particle surface. As an example, the spectrum of dodecylamine in deuterated chloroform (left) is compared to the spectrum of dodecylamine-stabilized ITO nanoparticles (right). The presence of the ITO nanoparticles results in changed intensity of the signal. The strong shift of the signals 1 and 2 which correspond to the two methyl groups next to the amine group, indicates an interaction of the amine with the ITO surface [20] (Fig. 7).

The binding strength between the stabilizer and the particle surface was determined using isothermal titration calorimetry (ITC). Therefore, the n-alkylamines of different chain lengths dissolved in chloroform were titrated with dispersions of ITO nanoparticles. Figure 8 shows the calculated enthalpy (ΔH) and entropy ($T\Delta S$) values for the titration process as well as the free energy (ΔG). Thereby, the binding enthalpy ΔH reflects the strength of the interactions between the n-alkylamines and the ITO surface relative to those existing with the solvent. In the case of the ITO/n-alkylamine systems, a change from enthalpically driven interactions to entropically driven interactions can be observed with an increase in the chain length. This is because the interactions between the stabilizer and the particle surface become more and more unspecific. Additionally, the increase in the chain

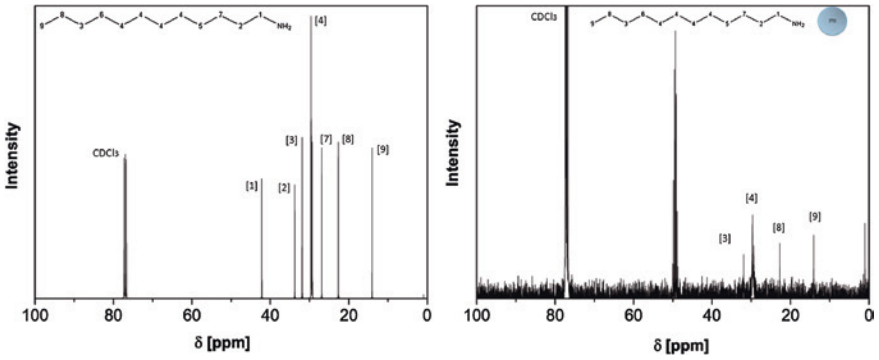

Fig. 7 ^{13}C-NMR spectra of docecylamine in $CDCl_3$ (*left*) and with dodecylamine stabilized ITO nanoparticles (*right*) [20]

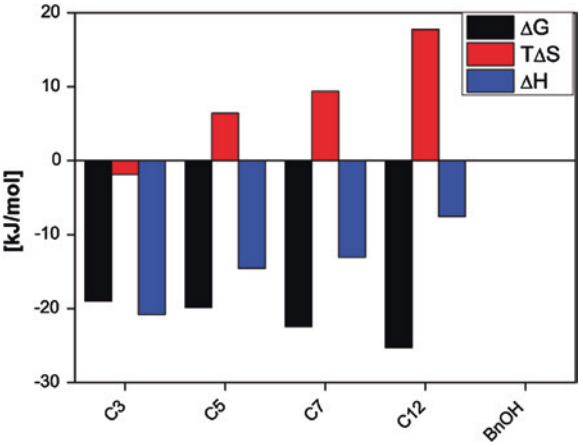

Fig. 8 Gibbs free energy, entropy and enthalpy values calculated with ITC for different chain length of n-alkylamines

length involves a decrease of the enthalpic contributions, so that the amine with the longest chain, dodecylamine, shows weak enthalpic interactions with the particle surface. Compared with the TiO_2 reference system, discussed in earlier works [21], the enthalpic contribution in the case of the ITO system is much lower, than for the TiO_2 reference system. Despite the weak interaction, the amino group of the stabilizer is still required to achieve the affinity to the particle surface. The addition of benzyl alcohol did not result in any detectable enthalpic effects. Details on these measurements and their evaluation can be found elsewhere [21].

Despite these weak interactions between stabilizer and particle surface, long-term stability of the particle system was observed [21]. Re-agglomeration of the ITO particles is possible by the addition of an anti-solvent to the particle dispersion. To investigate the re-agglomeration of the particles and the thereby incurred processes on their surface in detail, the amount of the stabilizer on the surface which was detected by solid-state ^{13}C-NMR is compared with TGA. ITO particles

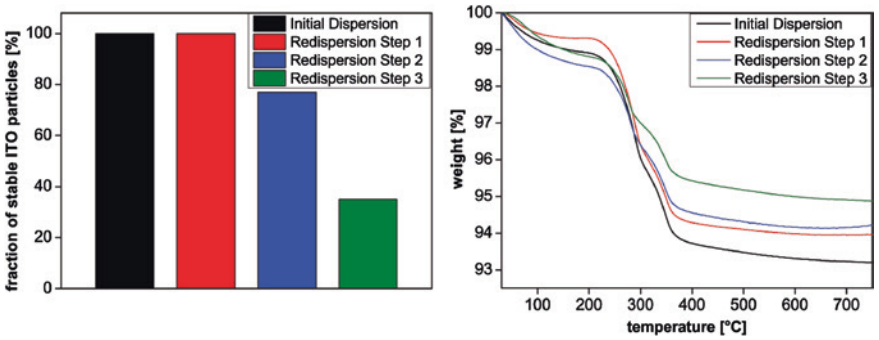

Fig. 9 Fraction of stable ITO particles (*left*) and TGA of ITO nanoparticles (*right*) before and after a number of precipitation-redispersion steps

stabilized with dodecylamine were precipitated by addition of an organic solvent (methanol) and redispersed three times. Figure 9 shows the results of TGA measurements (right) and the content of stable ITO particles before and after a number of precipitation-redispersion cycles (left).

The redispersion of the stabilized ITO nanoparticles leads to a decrease in stability of the nanoparticles, measured as decreased fraction of stable particles after the first redispersion cycle. This is due to the weak interactions between the stabilizer and the particle surface, as shown above by the ITC measurements. By precipitation and redispersion of the particles, some stabilizer molecules were detached from the surface because of the addition of the organic solvent. The detachment still small enough to achieve redispersion of the nanoparticles during the redispersion steps was verified by TGA and is plotted in Fig. 9 (right). In case of the first re-agglomeration step, the amount of bound stabilizer on the surface is still sufficient to achieve full redispersion of the nanoparticles. However, after three precipitation-redispersion cycles, the amount of coupled stabilizer molecules is so low that only 35 % of the particles are stable [20].

To investigate this process in detail, in cooperation Prof. Schmidt, University of Paderborn, solid-state ^{13}C-NMR spectroscopy was employed. Figure 10 shows the spectra of stabilized ITO nanoparticles after precipitation-redispersion cycles for 1, 2 and 3 times. The significant peaks are marked as peak 1, for the C-atoms of the alkyl chain, and peak 2, to assign benzyl alcohol. As already shown by TGA, an increase in the precipitation-redispersion steps leads to a decrease of the bound stabilizer on the particle surface. In contrast, the amount of benzyl alcohol remains constant over all steps.

In summary, the stabilization of ITO nanoparticles via n-alkylamines depends on the chain length and the amount of added stabilizer as well as on the stabilization time. The stabilization is based on the partial desorption of bound benzyl alcohol stemming from the synthesis and the concurrent adsorption of n-alkylamines, which only have a weak coordination to the surface. By addition of an anti-solvent, the precipitation and subsequent redispersion of the particles

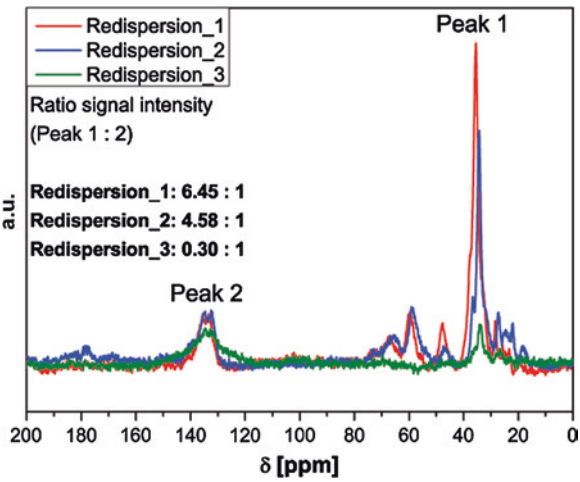

Fig. 10 Solid-state ^{13}C-NMR spectrum of redispersed ITO nanoparticles after different precipitation-redispersion steps

is possible, but the amount of stable particles decreases with every washing step. Nonetheless, the weak coordination between the stabilizer and the particle surface results in long-term stability of the ITO system.

3.4 Stabilization of ZrO_2 Nanoparticles with n-Carboxylic Acids

As a comparative model system, the stabilization of ZrO_2 with n-carboxylic acids of different chain lengths was investigated. Thereby, we have shown that the carboxylic acids bind to the particle surface via a selective interaction between the carboxylic acid group and the particle surface. Furthermore, a strong binding of the carboxylic acids to the ZrO_2 particle surface by the carboxylic group was determined by ^{13}C-NMR spectroscopy [17]. To show the influence of the strong interaction on the stabilization mechanism, a certain amount of the ZrO_2 nanoparticles were stabilized after synthesis under variation of the chain length and the added amount of stabilizer. The obtained solid content of stable ZrO_2 particles for carboxylic acids of different chain length is plotted in Fig. 11.

It should be noted, that due to the effect of the washing treatment, for the investigated system about 50 % of the ZrO_2 particles are stable without the addition of any stabilizer. As a result, only a small amount of the stabilizer is required to achieve full stability of the nanoparticles (stable fraction of 100 % of the used nanoparticles for the investigated setup). For low stabilizer-to-particle ratios, an increase in stable particles is registered for the stabilization with the short-chain stabilizer hexanoic acid (C_6). By using an amount higher than 0.05:1 (stabilizer: ZrO_2), almost 100 % of the particles are stable for all investigated carboxylic acids. The differences between the needed amounts of stabilizer to obtain

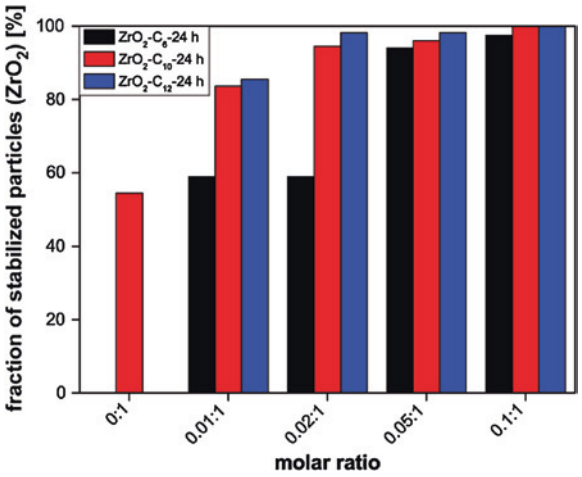

Fig. 11 Fraction of stabilized ZrO_2 nanoparticles depending on a variety of stabilizer concentration for carboxylic acids of different chain length; Reprinted with permission from [17]. Copyright 2012, American Chemical Society

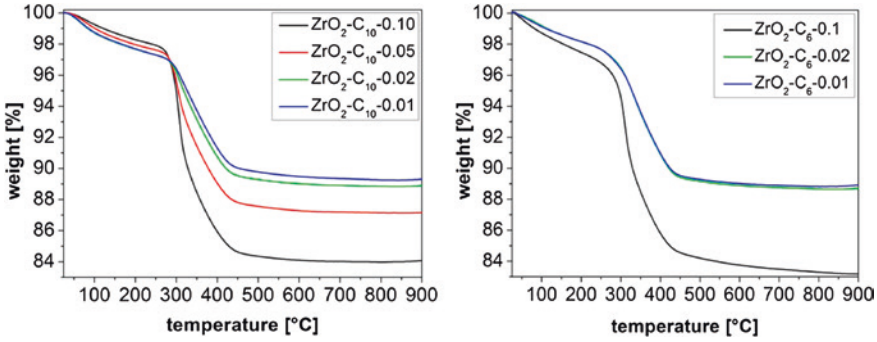

Fig. 12 TGA of ZrO_2 nanoparticles stabilized with the short-chain stabilizer hexanoic acid (*right*) and the long-chain stabilizer decanoic acid (*left*); Reprinted with permission from [17]. Copyright 2012, American Chemical Society

100 % stable particles of both particle systems can be attributed to the fact that, in the case of ZrO_2, a portion of benzyl alcohol is converted to benzoic acid, so that around 50 % of the particles are stable without any addition of the stabilizer. Furthermore, a stronger binding between the stabilizer and the particle surface leads to smaller amounts of needed stabilizer and less influences of the chain length on the stabilization process [17].

In order to investigate the adsorption and desorption processes on the particle surface in detail, TGA was carried out. Figure 12 shows the results of TGA measurements for the short-chain stabilizer hexanoic acid (right), and the long-chain stabilizer decanoic acid (left). For all measured samples, two main steps of weight

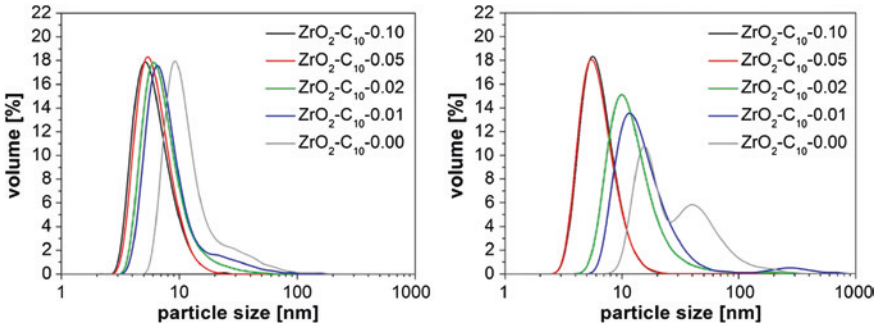

Fig. 13 Particle size distribution curves of stabilized ZrO_2 particles analyzed after 24 h (*left*) and after 1 month (*right*); Reprinted with permission from [17]. Copyright 2012, American Chemical Society

loss can be detected. The first step results from weakly-bound volatile solvents; the second step occurring at higher temperatures is attributed to the chemisorption of benzyl alcohol and its derivatives [17, 18]. Through the addition of the stabilizers with different chain lengths and in different amounts, an increase in the weight loss can be detected with TGA, which proves the presence of the stabilizer molecules on the particle surface. However, no significant differences are found for stabilizers with various chain lengths.

In order to show the influence of the chain length and the amount of added stabilizer on the long-term stability of ZrO_2 nanoparticles, we analyzed the produced dispersions via dynamic light scattering after 24 h and 1 month storage. The results of these experiments are plotted in Fig. 13 [17].

Above, a change in the particle size distribution after 1 month for a molar stabilizer-to-particle ratio lower than 0.05:1 is detected. Hence, for this system long-term stability is only achieved after the addition of higher amounts of stabilizer (i.e. molar ratio of 0.05:1 or higher) [17]. Furthermore, with the stabilization of ZrO_2 nanoparticles depending on the strong bindings, an unlimited number of precipitation-redispersion cycles are possible.

In conclusion, the long-term stability of ZrO_2 is achieved only after addition of a minimum concentration of a carboxylic acid as stabilizer. Thereby, no significant difference between stabilizers with different chain lengths could be identified. The peculiar surface chemistry of the ZrO_2 nanoparticles after the synthesis may explain the low amounts of needed stabilizer.

3.5 Modelling of Nanoparticle Stabilization

To predict the stabilization of nanoparticles by post-synthetic addition of stabilizers, an empirical model to describe the stabilization mechanisms on the

particle surface was developed. As shown in Figs. 5 and 11, the content of stable particles depends on the concentration of the stabilizer and reaches a saturation, which we postulate to be related to the saturation of stabilizer at the particle surface, to be mathematically expressed using the Langmuir equation. Following this equation, originally developed to describe the sorption of gas molecules on the surface of solid materials, but also being applicable to describe processes at solid-liquid interfaces, the ratio of stable particles as stability criterion was calculated. This is based on the assumptions that the stabilizer is chemically adsorbed as a molecular layer and that all binding sites are equal, so that only one molecule can be adsorbed to one binding site. The adsorption of the stabilizer moreover requires the desorption of benzyl alcohol and that there is no interaction between the molecules. Hence, the stability value (z) is a function of the maximum solid content (m_S) $\left[\frac{mass\ of\ the\ stable\ particle\ fraction}{total\ mass\ of\ all\ particles}\right]$ and the relative concentration (x) $\left[\frac{concentration\ stabilizer}{concentration\ particles}\right]$ of the used stabilizer. Thereby, the stability value can be described as the success of the stabilization, which reflects the maximum amount of particles which were stabilized to the primary particle size. Based on this function, the efficiency (E_S) of the respective stabilizer can be assessed and characterizes the potential of the particle-stabilizer system to achieve ideally 100 % stable particles by addition of a minimum stabilizer concentration. To be able to extend the model arbitrarily, the factor c as a function of the molecular weight, the time as well as the temperature was established.

$$stability\ value(z) = maximum\ solid\ content\ (m_S) \cdot \frac{concentration\ (x)^c}{concentration\ (x)^c + {}^1/_{efficiency\ (E_S)}}$$

Figure 14 shows the stability value, which is the solid content of the stable fraction, plotted over the concentration of the added n-alkylamines. To capture the influence of the chain length, the stability value was determined for different n-alkylamines. Furthermore, the maximum solid content as well as the efficiency are shown as functions of the molecular weight (chain-length) for a stabilization

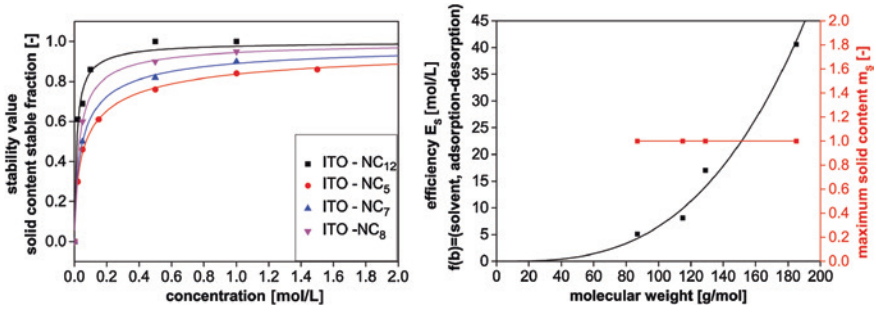

Fig. 14 Stability criterion for different stabilizers (*left*) and the efficiency of the systems depending on the molecular weight (*right*)

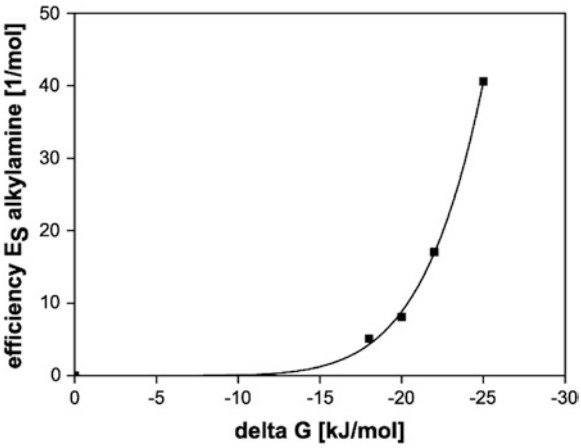

Fig. 15 Efficiency of the stabilization mechanism in relation to ΔG

time $t \rightarrow \infty$. Therefore, the maximum solid content is constant for all stabilizers and equals 1.

Due to the high number of free binding sites the solid content of the stable fraction increases almost linearly for low stabilizer concentrations. With an increase in the stabilizer concentration, the adsorption of the stabilizer and the desorption of the benzyl alcohol is hindered by conformational degrees and a decrease in free binding sites. This leads to a limitation of the diffusion and results in the formation of a plateau. As this plateau is reached, the stability criterion of 100 % stable particles is fulfilled. This is also shown in the efficiency of the different stabilizer systems (Fig. 14 right). Due to the strong influence of the chain length, the short-chain stabilizer amylamine shows a lower efficiency than the long-chain stabilizer dodecylamine. Combined with the results from ITC, the efficiency of the ITO/stabilizer systems is plotted over the free energy of stabilizer binding as shown in Fig. 15.

As already demonstrated in Fig. 8, the entropic effect and, thereby, the free energy ΔG of the whole system increases with longer chains. The correlation of the free energy to the efficiency of the system provides a comprehensive indication of the influences of dynamic and kinetic processes on the particle surface. The efficiency resembles the influences of the properties of the stabilizer molecules (chain-length, functional group, concentration); through ITC, influences of the binding strength could be coupled with the influence of solvent effects and the change of conformational degrees (entropic effects).

To compare both particle systems, the model was applied to the ZrO_2 system. In contrast to ITO, the stabilization of ZrO_2 is based on the addition of carboxylic acids. Furthermore, around 50 % of the particles are stable without adding stabilizer molecules; meaning that lower concentrations of the stabilizer are needed to achieve the stability value of 100 % stable particles. Figure 16 shows the implementation of the stabilization criterion on the stabilization process of ZrO_2 for carboxylic acids with different chain lengths.

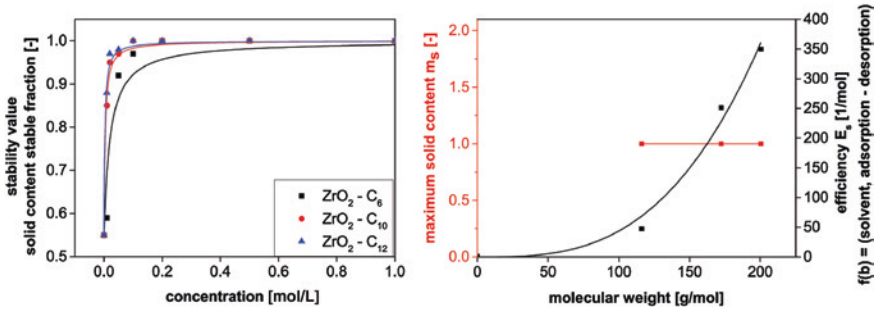

Fig. 16 Stability criterion for different carboxylic acids (*left*) and the efficiency of the systems depending on the molecular weight (*right*)

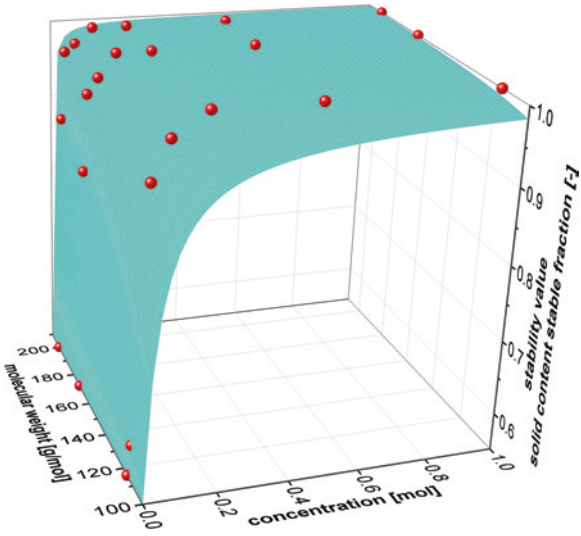

Fig. 17 3D plot of the stability value depending on the concentration and the molecular weight of the ZrO_2 system

Due to the strong interactions between the stabilizer and the particle surface, the stabilization is controlled by the amount of the stabilizer rather than the chain length of the stabilizer. Consequently, higher solid content and a sharper linear increase of the stability value for low stabilizer concentrations were achieved. This results in a higher efficiency with approximately 100 % stable particles in the ZrO_2 system and can be attributed to higher binding strength between the stabilizer and the particle surface in comparison to the ITO system.

To predict the stability value of different systems, a 3D plot based on the concentration, stability value and the molecular weight can be used and is shown in Fig. 17 for the ZrO_2 system.

The correlation of these parameters shows which factors are predominant for the stabilization. Furthermore, other parameters, such as the temperature, the

additional presence of different organics on the surface and the nature of the dispersion medium or different stabilization times, can be considered and extended via the empirical model.

4 Conclusion

The stabilization of metal oxide nanoparticles by addition of small-molecule stabilizers in a post-synthetic treatment was studied. By comparing two model systems, ZrO_2 and ITO, a number of differences between the stabilization mechanisms were elucidated. To stabilize ITO nanoparticles, weak interactions between the n-alkylamines and the particle surface were shown to be sufficient to achieve long-term stability of the system. Thereby, the stabilization depends on the concentration and the chain length of the stabilizer as well as on the stabilization time. Additionally, the stabilization of the particles is only achieved after some fractions of benzyl alcohol are desorbed. This interaction between the adsorption of stabilizer and the desorption of benzyl alcohol determines the stabilization mechanism.

In the case of ZrO_2 strong bonds between the stabilizer and the surface were detected and resulted in a higher efficiency of the system. In essence, the stabilization of ZrO_2 nanoparticles depends on the concentration of the added stabilizer to achieve long-term stability. Furthermore, due to the strong bonds a full redispersion of the particles is possible.

The differences between the stabilization mechanisms in the two systems may be explained by the formation of benzoic acid on the ZrO_2 surface as well as on the different binding strength, strong binding between the carboxylic acids and the ZrO_2 nanoparticle surface and weak interactions between the n-alkylamines and the ITO particles. Despite these differences, the developed empirical model can be used, to describe and predict surface processes and influences on the stabilization mechanism for different particle systems. Depending on the selected parameters, different influences, such as the temperature or the stabilization time, can be considered and implemented in the model. This allows arbitrary considerations of the model to predict particle-stabilizer-solvent interactions in a complex organic environment typical for nanoparticles prepared in hot organic media. In future the applicability of the model for different stabilization processes should investigate.

Acknowledgments The authors gratefully acknowledge the financial support provided by the German Research Foundation within SPP 1273 grants GA 1492/4-1 and 2. Furthermore, the authors acknowledge Dr. D. Vollmer and K. J. Chiad from the MPI Mainz for the isothermal titration calorimetry, Prof. Dr. C. Schmidt and M. Kube from the University Paderborn for the solid-state-^{13}C-NMR spectroscopy, Dr. K. Ibrom and P. Holba-Schulz from the TU Braunschweig for the NMR spectroscopy measurements, Dr. H.-O. Burmeister, S. Meyer and P. Reich for the elemental analysis as well as Dr.-Ing. D. Segets and Prof. Dr.-Ing. W. Peukert from the Institute of Particle Technology (LFG Erlangen) and Dr.-Ing. C. Schilde and Prof. Dr.-Ing. A. Kwade for discussions within the project.

References

1. Ginley DS, Bright C (2000) Transparent conducting oxides. MRS Bull 25:15–18
2. Minami T (2005) Transparent conducting oxide semiconductors for transparent electrodes. Semicond Sci Technol 20:S35–S44
3. Ba J et al (2006) Nonaqueous synthesis of uniform indium tin oxide nanocrystals and their electrical conductivity in dependence of the tin oxide concentration. Chem Mater 18:2848–2854
4. Tanabe K (1985) Surface and catalytic properties of ZrO_2. Mater Chem Phys 13:347–364
5. Garvie RC et al (1975) Ceramic steel?. Nature 258:703–704
6. Wilk GD et al (2001) High-k gate dielectrics: Current status and materials properties considerations. J Appl Phys 89:5243
7. Heuer AH, Hobbs LW (1981) Science and technology of zirconia, American Ceramic Society, vol. 3. Columbus and Ohio
8. Inoue M et al (1993) Novel synthetic method for the catalytic use of thermally stable zirconia: thermal decomposition of zirconium alkoxides in organic media. Appl Catal A 97:L25–L30
9. Joo J et al (2003) Multigram scale synthesis and characterization of monodisperse tetragonal zirconia nanocrystals. J Am Chem Soc 125:6553–6557
10. Buchanan RC, Pope S (1983) Optical and electrical properties of yttria stabilized zirconia (YSZ) crystals. J Electrochem Soc 130:962
11. Krell A et al (2009) Transparent compact ceramics: Inherent physical issues. Opt Mater 31:1144–1150
12. Robertson J (2006) High dielectric constant gate oxides for metal oxide si transistors. Rep Prog Phys 69:327–396
13. Taroata D et al (2012) High integration density capacitors directly integrated in single copper layer of printed circuit boards. IEEE Trans Dielectr Electr Insul 19:298–304
14. Garnweitner G (2007) Large-scale synthesis of organophilic zirconia nanoparticles and their application in organic-inorganic nanocomposites for efficient volume holography. Small 3(9):1626–1632
15. Tsedev N, Garnweitner G (2008) Surface modification of ZrO_2 nanoparticles as functional component in optical nanocomposite device. Mater Res Soc Symp Proc 1076:K05–03
16. Cheema TA, Garnweitner G (2014) Phase-controlled synthesis of ZrO_2 nanoparticles for highly transparent dielectric thin films. Cryst Eng Commun 16:3366
17. Grote C et al (2012) Comparative study of ligand binding during the postsynthetic stabilization of metal oxide nanoparticles. Langmuir 28:14395–14404
18. Zhou S et al (2007) Dispersion behavior of zirconia nanocrystals and their surface functionalization with vinyl group-containing ligands. Langmuir 23:9178–9187
19. Pinna N et al (2005) Synthesis of yttria-based crystalline and lamellar nanostructures and their formation mechanism. Small 1(1):112–121
20. Zellmer S, Garnweitner G (2013) Stabilization of metal oxide nanoparticles by binding of molecular ligands. In: PARTEC—international congress on particle technology, proceedings, Nuremberg, 23–25 April 2013
21. Grote C et al (2012) Unspecific ligand binding yielding stable colloidal ITO-nanoparticle dispersions. Chem Commun 48:1464–1466
22. Russel WB et al (1989) Colloidal dispersions. Cambridge University Press, Cambridge
23. Heller W, Pugh TL (1954) “Steric protection” of hydrophobic colloidal particles by adsorption of flexible macromolecules. J Chem Phys 22:1778
24. Tripathy SS, Raichur AM (2008) Dispersibility of barium titanate suspension in the presence of polyelectrolytes: A Review. J Dispersion Sci Technol 29:230–239
25. Overbeek JTG (1966) Colloid stability in aqueous and non-aqueous media. Discuss Faraday Soc 42:7–13

26. Boal AK et al (2002) Monolayer exchange chemistry of γ-Fe_2O_3 nanoparticles. Chem Mater 14:2628–2636
27. Bergström L et al (1992) Consolidation behavior of flocculated alumina suspensions. J Am Ceram Soc 75:3305–3314
28. Bell NS et al (2005) Rheological properties of nanopowder alumina coated with adsorbed fatty acids. J Colloid Interface Sci 287:94–106
29. Siffert B (1994) Location of the shear plane in the electric double layer in an organic medium. J Colloid Interface Sci 163:327–333
30. Sun D et al (2007) Purification and stabilization of colloidal ZnO nanoparticles in methanol. J Sol-Gel Sci Technol 43(2):237–243
31. Marczak R et al (2010) Optimum between purification and colloidal stability of ZnO nanoparticles. Adv Powder Technol 21(1):41–49
32. Segets D et al (2011) Experimental and theoretical studies of the colloidal stability of nanoparticles-a general interpretation based on stability maps. ACS Nano 5(6):4658–4669
33. Garnweitner G (2010) Small molecule stabilization. In: Segewitz L, Petrowsky M (eds) Polymer aging, Stabilizers and Amphipilic Block Copolymers